Dynamic Intensity Model Calculation of Vibronic Oscillator Strengths for $Cs_2NaNdCl_6$: A Molecular Dynamics Study

Lixin Ning,*,† Sverker Edvardsson,† and Daniel Åberg‡

Department of Physical Electronics and Photonics, Mid Sweden University, S-851 70, Sundsvall, Sweden, and Lawrence Livermore National Laboratory, Livermore, California 94551

Received: May 12, 2006; In Final Form: August 23, 2006

We present here a dynamic intensity model calculation of vibronic oscillator strengths for the $Cs_2NaNdCl_6$ compound by applying the method of molecular-dynamics simulation (MDS). The force field parameters used for the MDS reproduce the structure and several vibrational frequencies of $Cs_2NaNdCl_6$ very well. Both the static-coupling (SC) and dynamic-coupling (DC) mechanisms are taken into account for the intensity parameter calculations, in which the effective point charges and isotropic polarizabilities are optimized with respect to experimental energy levels. A comparison of intensity parameters and vibronic oscillator strengths between the two individual mechanisms indicates that the DC mechanism is operative. The calculated vibronic oscillator strengths for the combined SC and DC mechanism agree quite well with the available experimental values.

1. Introduction

The optical spectra of trivalent rare-earth (RE) ions in crystals often show vibronic features with small intensities determined by the strength of electron−lattice coupling. Consequently, the vibronic intensities of RE spectra are of special interest not only from a fundamental point of view, but also from an applied one, for example, in the applications of RE ions in laser materials, fiber amplifiers for telecommunication, or luminescent materials.

There are several theoretical models in the description of vibronic intensities of RE ions. The vibronic coupling model of Faulkner and Richardson[1,2] has been most widely applied to the calculation of vibronic intensities of the $Cs_2NaLnCl_6$ systems. However, this model involves complexity in the numerical evaluation of derivatives of crystal-field parameters (CFP) with respect to the relevant normal coordinates. Judd[3] worked out a similar approach to the $LnCl_6$ octahedron using tensor techniques. Stavola et al.[4] developed a cooperative model to study the vibronic intensity involving an electronic 4f−4f transition and a simultaneous vibrational transition of a nearby ligand molecule. Later, Dexpert-Ghys and Auzel[5] improved this model by considering the contribution of Franck−Condon replicas to the vibronic intensity of RE ions sitting in noncentrosymmetric sites. MDS has been utilized many times to study optical properties of RE ions in amorphous systems.[6−12] In these systems, the chemical environments surrounding the RE ions are very different, and thus the zero phonon oscillator strengths must be calculated for each chemical environment. For these cases, MDS has proved to be a convenient way for the construction of physically sound environments surrounding the RE ions. On the other hand, the recent presentation of the dynamic intensity model demonstrated that MDS can also be applied to calculate vibronic transitions in crystalline systems.[13] In our opinion, this approach can simplify these type of calculations tremendously. It is thus of interest to apply the dynamic intensity model together with MDS to compute vibronic intensities of RE ions in real materials. A crystalline compound, $Cs_2NaNdCl_6$, has been selected for the present investigation. In this centrosymmetric system, the zero phonon 4f−4f transitions are forbidden, and thus, the observed oscillator strengths are mainly those of vibronic and magnetic dipole transitions in origin. The absorption spectra of this compound have been measured at room temperature by several groups[14−16] and the experimental values of the oscillator strengths have been tabulated by Strek et al.[15] Therefore, a calculation of vibronic oscillator strengths for this compound can be considered to be a good test for the dynamic intensity model combined with the MDS method. MDS only deals with classical dynamics so the complexity associated with differentiation of normal coordinates and access to the exact vibrational wave functions are avoided. In this work, a brief description of the dynamic intensity model is outlined in section 2. The MDS calculations of the $Cs_2NaNdCl_6$ compound and then the intensity parameter calculations for the MDS-generated Nd-ion environments are described in section 3. The main results of calculations are tabulated and discussed in section 4, with the final conclusions collected in section 5.

2. Intensities from the Dynamic Intensity Model

If we adopt the Judd−Ofelt approximation, the integrated isotropic oscillator strength of the electric dipole absorption from an initial multiplet $|[\alpha_i S_i L_i]J_i\rangle$ to a final multiplet $|[\alpha_f S_f L_f]J_f\rangle$ within $4f^N$ configuration may be written as[17,18]

$$P_{if}^{ED} = \frac{8\pi^2 m_e c\bar{\nu}_{if}}{3h(2J_i+1)}\frac{(n^2+2)^2}{9n}\sum_{\lambda_{tp}}\frac{|A_{tp}^{\lambda}|^2}{2\lambda+1}| \times \langle 4f^N[\alpha_f S_f L_f]J_f||U^{(\lambda)}||4f^N[\alpha_i S_i L_i]J_i\rangle|^2 \quad (1)$$

with $\lambda = 2, 4, 6$, $t = \lambda, \pm 1$, and p restricted by the site symmetry

* Corresponding author.
† Department of Physical Electronics and Photonics, Mid Sweden University.
‡ Lawrence Livermore National Laboratory.

10.1021/jp062930w CCC: $33.50
Published on Web 10/04/2006

of the RE ion. m_e, c, $\bar{\nu}_{if}$, h, and n are the electron mass, the light velocity in a vacuum, the transition wavenumber (in units of cm^{-1}), Planck's constant, and the refractive index of the material, respectively. The initial and final multiplets are labeled by their principal components in the intermediate coupling scheme. In the following, the spectral term $4f^N[\alpha SL]$ will be abbreviated to the symbol ψ. The A^{λ}_{tp} parameters contain structural information about the chemical environment as well as intrinsic electronic properties of the RE ion.

In the standard Judd−Ofelt theory, Ω_λ are the intensity parameters of interest, and are related to the A^{λ}_{tp} parameters as follows:

$$\Omega_\lambda = \frac{1}{2\lambda+1}\sum_{t,p}|A_{tp}{}^{\lambda}|^2$$

Given the crystallographic positions $\vec{R}_L$ of the ligands, the A^{λ}_{tp} parameters may be calculated by applying some appropriate physical model. For convenience, it is assumed that the center of coordinate system is in the site of the RE ion. At temperatures considerably above 0 K, the RE ion experiences significant fluctuations from its chemical environment. These variations are due to the dynamics alone, and result in a dynamical crystal-field at the given RE site. In the present work, the fluctuating environments surrounding the RE ion are obtained by using the MDS technique. The oscillator strength (the observable in statistical mechanics), which is the experimental property of interest, is obtained by a simple average of the squared intensity parameters $|A^{\lambda}_{tp}|^2$ [see eq 1]. Namely, the $|A^{\lambda}_{tp}|^2$ are computed for each MDS-generated environment of the RE ion, and finally averaged for these environments to obtain the appropriate $\langle|A^{\lambda}_{tp}|^2\rangle$ intensity parameter. The observed integrated isotropic oscillator strength of a $|\psi_i J_i\rangle \rightarrow |\psi_f J_f\rangle$ band is then simply given by

$$P^{ED}_{if} = \frac{8\pi^2 m_e c\bar{\nu}_{if}}{3h(2J_i+1)}\frac{(n^2+2)^2}{9n}\sum_{\lambda,tp}\frac{\langle|A^{\lambda}_{tp}|^2\rangle}{2\lambda+1}|\langle\psi_f J_f\|U^{\lambda}\|\psi_i J_i\rangle|^2 \quad (2)$$

The computed oscillator strength from this approach encompasses the contributions from both zero and nonzero phonon transitions. This is analogous to the static and dynamic part of the $\langle|A^{\lambda}_{tp}|^2\rangle$ parameters in the quantum mechanical approach (Taylor expansion), respectively. Although our approach is different from a quantum mechanical treatment, the final results are in fact essentially identical, provided that the method is applied for a reasonably high temperature. The basic concept of calculating vibronic oscillator strengths using relatively simple MDS was recently described in ref 13. For the $Cs_2NaNdCl_6$ compound, the site symmetry of the Nd ion is O_h, and hence the static t-odd intensity parameters are all zero. Thus, for the present compound, the $\langle|A^{\lambda}_{tp}|^2\rangle$ parameters consist of only the dynamic contributions corresponding to nonzero phonon transitions, and these are conveniently obtained by using the MDS approach.

3. Calculations

3.1 Molecular-Dynamics Simulation. The cubic unit cell of the compound $Cs_2NaNdCl_6$ contains four formula units. The structure was sketched in Figure 1 of ref 19. It crystallizes in the face-center cubic space group $Fm3m$ (No. 225) with 40 atoms in the cubic unit cell. The Nd ions occupy the 4a sites (O_h point symmetry) in 6-coordination with Cl. The Cl ions occupy 24(e) sites (C_{4v} point symmetry) whose exact locations depend on the structure parameter x. The Cs and Na occupy the 8c and 4b sites with T_d and O_h point symmetries, respectively. The lattice constant for $Cs_2NaNdCl_6$ is 10.8894 Å[20] and the structure parameter is approximately $x = 0.245$.[21]

The force field employed for this compound is composed of a Buckingham potential to model the short-range Pauli repulsion, the leading term of dispersion energy, and the Coulomb interaction:

$$E_{ij} = A_{ij}\exp(-r_{ij}/\rho_{ij}) - C_{ij}r_{ij}{}^{-6} + q_i q_j/r_{ij}$$

Here A_{ij}, ρ_{ij} and C_{ij} are empirically determined parameters. The ionic charges q_i were set equal to their formal values.

The polarizabilities of the ions have also been included by using the shell model.[22] A mass-less shell of charge Y, on which all interatomic potentials act, is coupled by a harmonic spring to a core, i.e.

$$E_{\text{core-shell}} = \frac{1}{2}k_2 r^2$$

resulting in an environment-dependent ion polarizability, and k_2 is again an empirical parameter. For $Cs_2NaNdCl_6$, only the Cl ion has been treated as polarizable in the calculation of the polarization contributions to the inter-ionic forces. The polarization contributions of the other Cs, Na, and Nd ions were assumed to be negligible, since they are located in environments with high symmetries (with negligible electric fields).[23] All the MD calculations have been performed using the program GULP.[24]

The short-range interaction terms introduced by the model describe Na−Cl, Nd−Cl, Cs−Cl, and Cl−Cl interactions. The parameters for the Cs−Cl and Cl−Cl interactions were assumed to be transferable, and taken from the work of Sangster et al.[25] Model parameters that include the short-range interaction parameters for Na−Cl and Nd−Cl interactions, along with the shell charge and spring constant of the Cl ion, were fitted to the lattice structures (i.e., the lattice constant and the structure parameter) and several vibrational frequencies at 300 K. These frequencies are well separated from the others, and include the zero-frequencies of the lowest triply degenerate T_{1u} vibrational mode (acoustic mode) at the Γ point of the Brillouin zone, the highest frequency (281 cm^{-1}) of the only nondegenerate A_{1g} vibrational mode at the Γ point, and the frequencies (220 cm^{-1}) of the only doubly degenerate E_g vibrational mode at the Γ point.[26] The relaxed fitting algorithm was used in all parameter determinations.[27] The final interatomic potential parameters obtained are given in Table 1. These parameters reproduce the crystalline properties of $Cs_2NaNdCl_6$ very well, as can been seen in Table 2.

A simulation box of $3 \times 3 \times 3$ unit cells has been selected, which contains 1080 atoms including 108 Nd ions. The simulations were first equilibrated and then continued for 6000 time steps with $\Delta t = 2.0$ fs to collect the data of Nd-ion environments for the subsequent calculation of squared intensity parameters. Specific details on the MDS technique and the calculations may be found in ref 24.

3.2. Averaging of Intensity Parameters. In order to calculate the $|A^{\lambda}_{tp}|^2$ intensity parameters for each MDS-generated Nd-ion environment, we used a simple physical model. Two intensity mechanisms were considered, namely the SC and DC mechanisms,[28] and the relevant A^{λ}_{tp} parameters are then expressed as[6]

$$A^{\lambda}_{tp}[SC] = -A_{tp}\Xi(t,\lambda)(2\lambda+1)/\sqrt{2t+1} \quad (3)$$

TABLE 1: Short-Range Potential and Shell Model Parameters for $Cs_2NaNdCl_6$ (c = Core; s = Shell)

(a) Short-Range Potential Parameters

	A_{ij} (eV)	ρ_{ij} (Å)	C_{ij} (eV Å^6)
Nd_c-Nd_c	0.0		0.0
Nd_c-Na_c	0.0		0.0
Nd_c-Cs_c	0.0		0.0
Nd_c-Cl_s	18141.1[a]	0.242[a]	0.0
Na_c-Na_c	0.0		0.0
Na_c-Cs_c	0.0		0.0
Na_c-Cl_s	4928.65[a]	0.250[a]	0.0
Cs_c-Cs_c	0.0		0.0
Cs_c-Cl_s	4717.0[b]	0.346[b]	0.0
Cl_s-Cl_s	3361.0[b]	0.356[b]	193.9[b]

(b) Shell Model Parameters

	k_2 (eV Å^{-2})	Y (e)
Cl_c-Cl_s	29.35[a]	−1.1685[a]

[a] Fitted values. [b] Reference 25.

TABLE 2: Calculated Properties for $Cs_2NaNdCl_6$ at 300 K

	expt	calcd
lattice constant a, Å	10.8894 [a]	10.8471
the structural parameter x for Cl	0.245 [b]	core: 0.229279 shell: 0.227510
the frequencies (cm^{-1}) of vibrational modes at Γ point		
T_{1u} (acoustic mode)	0	0
E_g	220	207
A_{1g}	281	277

[a] Reference 20. [b] Reference 21.

and

$$A_{tp}^{\lambda}[DC] = -\delta_{t,\lambda+1}\, 7\sqrt{(2\lambda+1)(\lambda+1)}\langle 4f|r^{\lambda}|4f\rangle(1-\sigma_{\lambda}) \begin{pmatrix} 3 & \lambda & 3 \\ 0 & 0 & 0 \end{pmatrix} \times \sum_{L}(-1)^{p} C_{-p}^{(\lambda+1)}(\Omega_L)\bar{\alpha}_L R_L^{-(\lambda+2)} \quad (4)$$

respectively, where R_L and Ω_L are spherical coordinates for a ligand L having the effective point charge q_L and the effective isotropic polarizability $\bar{\alpha}_L$. The applied values for shielding factors σ_λ and radial integrals $\langle 4f|r^{\lambda}|4f\rangle$ can be found in ref 12. The $\Xi(t,\lambda)$ in eq 3, defined by eq 14 in ref 29, involve a sum over interconfigurational radial integrals and energy differences, and these values were computed by applying the perturbed functions approach; see ref 13. In eq 3, the t-odd A_{tp} parameters have been calculated using the self-consistent electrostatic multipole model:[30−32]

$$A_{tp} = (-1)^{p+1}\int n(\vec{R})R^{-(t+1)}C_{-p}^{(t)}(\Omega)dV \approx (-1)^{p+1}\sum_{L}\{q_L R_L^{-(t+1)} - (t+1)\bar{\alpha}_L \vec{E}_L\cdot\vec{e}_L R_L^{-(t+2)}\}C_{-p}^{(t)}(\Omega_L) \quad (5)$$

Here $n(\vec{R})$is the external charge density, $\vec{E}_L$ is the electric field at the ligand site L, $\vec{e}_L$ is the unit vector from the Nd ion to the ligand site L. For each MDS-generated environment, the electric fields $\vec{E}_L$ at the atomic positions were computed self-consistently, see ref 30. The summations were carried out for the surrounding ligands to a cutoff distance R_{cut} = 30 Å. The effective point charges q_L and isotropic polarizabilities $\bar{\alpha}_L$ in eqs 4 and 5 have been determined from optimization of a selected model cluster with a Nd ion at the origin, with respect to experimental crystal-field energy levels of the $Cs_2NaNdCl_6$ crystal.[33] The radius of this model cluster is 30 Å, with the well-defined crystallographic coordinate system for $Cs_2NaNdCl_6$. The t-even A_{tp} parameters required for energy level calculations were evaluated according to eq 5, wherein the electric fields at ligand sites were computed self-consistently. Optimization was performed by varying the effective point charges q_L and polarizabilities $\bar{\alpha}_L$ within physical ranges. The relation between the standard t-even B_{tp} and A_{tp} is $B_{tp} = \rho_t A_{tp}$ (t = 4, 6 and $p = 0, \pm 4$), where ρ_t accounts for an effective expansion of the radial f function and shielding, and were also optimized within certain allowed ranges. The effective Hamiltonian

$$H_{\text{eff}} = \sum_{k=2,4,6} f_k F^k + \sum_i \zeta l_i\cdot s_i + \alpha L^2 + \beta G(G_2) + \gamma G(R_7) + \sum_{i=2,3,4,6,7,8} t_i T^i + \sum_i \sum_{tp} B_{tp} C_{tp}(\Omega_i) \quad (6)$$

was then repeatedly diagonalized using the software *lanthanide*[34] until optimized stark level energies were obtained. All parameters (i.e., F^2, F^4, F^6, ζ, α, β, γ, T^2, T^3, T^4, T^6, T^7, T^8, q_L, $\bar{\alpha}_L$, and ρ_t) were varied simultaneously. Because of the high site symmetries of the Cs, Na, and Nd ions, the electric fields at these sites are zero. Thus, as in the case of MDS, only the polarizabilities of Cl ions (with C_{4v} site symmetry) were considered. In addition, $2q_{Cs} + q_{Na} + q_{Nd} + 6q_{Cl} = 0$ is required for neutrality. This condition reduces the number of free parameters to 20. The resulting optimized parameter values are listed in Table 3. The standard deviation in this work is defined as

$$\sigma = \left(\sum_{i}^{N}(E_{i,\text{fit}} - E_{i,\text{exp}})^2/N\right)^{1/2}$$

where N denotes the total number of energy levels included in the energy level fit. Quite a good fit within this model framework was obtained: σ = 23.2 cm^{-1}, which is comparable to the value σ = 21.5 cm^{-1} in ref 33, where instead a direct variation of the B_{tp}'s were carried out. The optimized effective point charges and the isotropic polarizability for the Cl ion were then substituted into Eqs. (3−5) to calculate the intensity parameters for the MDS-generated Nd-ion environments. In addition, the optimized free-ion parameters listed in Table 3 have been applied to calculate the corresponding squared reduced matrix elements (SRMEs), $|\langle\psi_f J_f||U^{(\lambda)}||\psi_i J_i\rangle|^2$, for the oscillator strength calculations [see eq 2]. The values for the SRMEs are listed in Table 4.

In both the static and dynamic coupling models, the forms of interaction have been assumed to be electrostatic in character although effects of overlap between the charge densities of the central RE ion and ligands are partly simulated through the use of optimized effective point charges and polarizabilities. The total squared intensity parameter for the combined SC and DC mechanism is written

$$|A_{tp}^{\lambda}|^2 = |A_{tp}^{\lambda}[SC] + A_{tp}^{\lambda}[DC]|^2 \quad (7)$$

These are the quantities needed to be evaluated for each MDS-generated chemical environment surrounding a given Nd ion. To study the contributions to the $|A_{tp}^{\lambda}|^2$ parameter from the individual SC and DC mechanisms, the $|A_{tp}^{\lambda}[SC]|^2$ and $|A_{tp}^{\lambda}[DC]|^2$ intensity parameters were also computed separately. All the intensity parameters were finally averaged over all the MDS-generated Nd-ion environments and substituted into eq 2 to give the integrated vibronic oscillator strengths. Besides the

TABLE 3: Optimized Energy Parameters for $Cs_2NaNdCl_6$,[a] Where F^k, ξ, α, β, γ, T^i, and σ Are in Units of cm^{-1}

parameter		parameter		parameter		parameter	
F^2	71089.9	β	−919.1	T_6	−281.5	q_{Cs}	0.792 (1.0)
F^4	53385.2	γ	1619.7	T_7	519.9	q_{Na}	0.903 (1.0)
F^6	35156.4	T_2	270.3	T_8	313.2	q_{Nd}	2.823 (3.0)
ξ	870.9	T_3	90.8	ρ_4	3.54	q_{Cl}	−0.885 (−1.0)
α	24.6	T_4	98.1	ρ_6	53.8	$\bar{\alpha}_{Cl}$	2.205 (2.694)
N	33	σ	23.2	B_{40}	1937.5	B_{60}	301.7

[a] The optimized isotropic polarizability of the Cl ion and the parameter ρ_t are expressed in $Å^3$ and atomic units, respectively. For comparison, we also list in the parentheses formal charges and the in-crystal polarizability of the Cl ion by Schmidt et al.[35] The B_{tp} parameters (in cm^{-1}) were obtained from $B_{tp} = \rho_t A_{tp}$.

TABLE 4: Squared Reduced Matrix Elements of $U^{(\lambda)}$ for $Cs_2NaNdCl_6$.

		$\lvert\langle\psi_f J_f \lvert\lvert U^{(\lambda)} \rvert\rvert {}^4I_{9/2}\rangle\rvert^2$		
$\psi_f J_f$	calculated energy (cm^{-1} above $^4I_{9/2}$)	$\lambda = 2$	$\lambda = 4$	$\lambda = 6$
$^4F_{3/2}$	11 186	0	0.2283	0.0580
$^4F_{5/2}$	12 225	0.0009	0.2363	0.3978
$^2H_{9/2}$	12 388	0.0093	0.0084	0.1148
$^4F_{7/2}$	13 203	0.0010	0.0429	0.4241
$^4S_{3/2}$	13 604	0	0.0023	0.2321
$^4G_{5/2}$	16 738	0.8978	0.4097	0.0375
$^2G_{7/2}$	16 970	0.0800	0.1935	0.0353
$^4G_{7/2}$	18 683	0.0508	0.1477	0.0518
$^4G_{9/2}$	19 103	0.0048	0.0615	0.0420
$^2K_{13/2}$	19 304	0.0072	0.0002	0.0321
$^2G_{9/2}$	20 738	0.0009	0.0138	0.0125
$^2D_{3/2}$	20 876	0	0.0229	0.0004
$^4G_{11/2}$	21 088	0	0.0051	0.0079
$^2K_{15/2}$	21 270	0	0.0051	0.0147
$^2P_{1/2}$	22 835	0	0.0412	0
$^4D_{3/2}$	27 557	0	0.1955	0.0173
$^4D_{5/2}$	27 611	0	0.0562	0.0275
$^4D_{1/2}$	28 105	0	0.2539	0
$^2I_{11/2}$	28 991	0.0047	0.0147	0.0036
$^2L_{15/2}$	29 553	0	0.0250	0.0102

vibronic transitions, the contributions from magnetic dipole transitions should also be included in the integrated oscillator strength of a $|\psi_i J_i\rangle \rightarrow |\psi_f J_f\rangle$ band in a comparison with experiment. However, for the spectral region (10 000−30 000 cm^{-1}) studied in this work, the magnetic dipole transitions are in general at least an order of magnitude less intense than the electric dipole transitions[36]. This was also confirmed in this study and thus neglected.

4. Results and Discussion

Calculated intensity parameters are presented in Table 5. From the table, we can see that each value of the total average $\langle|A^\lambda_{tp}|^2\rangle$ intensity parameters with $t = \lambda + 1$, is smaller than the corresponding value of the sum $\langle|A^\lambda_{tp}[SC]|^2\rangle + \langle|A^\lambda_{tp}[DC]|^2\rangle$. This is explained by the fact that the SC and DC mechanisms contribute to the total average intensity parameters with opposite signs [see eq 7], which is also consistent with earlier works.[37−39] Moreover, also for the $t=\lambda+1$ parameters, the $\langle|A^\lambda_{tp}[DC]|^2\rangle$ parameter values are much larger than the corresponding $\langle|A^\lambda_{tp}[SC]|^2\rangle$values, which suggests that the DC mechanism in general cannot be neglected. By using the intensity parameters given in Table 5, the vibronic oscillator strengths P were evaluated by using eq 2 for those transitions of $Cs_2NaNdCl_6$ for which experimental data exist.[15] The value of the refractive index has been taken to be 1.55 in these calculations.[40] In Table 6, the results are separated into eight groups to facilitate comparison with the experimental values in the last column. The calculated vibronic oscillator strengths for the individual SC and DC mechanisms are presented in the third and fourth columns (columns SC and DC), respectively. Comparison of the values between these two columns reveals that the DC mechanism is operative in the contributions to the oscillator strengths. The same conclusions on the relative importance of the SC and DC contributions to the vibronic intensities have also been made by Faulkner et al.[1,2] and Judd,[3] although their models are different from our approach. From the total average intensity parameters in Table 5, the vibronic oscillator strengths for the combined SC and DC mechanism are also given. These results are listed in column A of Table 6 and plotted in Figure 1. The overall agreement between the model calculations and experiment is quite reasonable. The differences, besides uncertainties in the experimental values, could be due to, for example: J-mixing effects, overlap of the charge densities between the Nd and Cl ions, and electron correlation effects, as discussed briefly in the following.

One of the assumptions on which the validity of eq 2 are based, is that the crystal-field-induced mixing among different J multiplets can be neglected. These J-mixing effects on the calculated vibronic oscillator strengths of this study may be evaluated using a revised Judd−Ofelt theory proposed by Xia et al.,[41] in which the $|\langle\psi_f J_f||U^{(\lambda)}||\psi_i J_i\rangle|^2$ in eq 2 is replaced by

$$\sum_{\psi'_f J'_f \psi'_i J'_i} \frac{|a(\psi_f J_f, \psi'_f J'_f)|^2}{2J'_f + 1} \frac{|a(\psi_i J_i, \psi'_i J'_i)|^2}{2J'_i + 1} |\langle\psi'_f J'_f||U^{(\lambda)}||\psi'_i J'_i\rangle|^2 \quad (8)$$

where the $|a(\psi J, \psi' J')|^2$ coefficients may be calculated by using Eqs. (10−12) in ref 41 together with the even CFP (B_{tp}) values listed in Table 3, and the calculated energies and SRME values in Table 4. However, for the $^4I_{9/2} \rightarrow {}^4D_{3/2}$, $^4D_{5/2}$ transitions, the nondegenerate perturbation method employed in ref 41 cannot be used since the $^4D_{3/2}$ and $^4D_{5/2}$ energy levels are nearly degenerate, as shown by the energies in Table 4. Instead, we derived the J-mixing coefficients between these two multiplets by using the crystal-field eigenvectors from the energy matrix of the effective Hamiltonian in eq 6. The final results for the eight groups of transitions are listed in column B of Table 6. The results are slightly improved with respect to the experimental values in comparison with those in column A (without J-mixing). An inspection of the results in Table 6 shows that, except for the fourth and eighth groups of transitions, the vibronic oscillator strengths are, to greater or lesser extent, smaller than the corresponding experimental values. It may be linked to the fact that the overlap of charge densities between the RE ions and its ligands has not really been accounted for in the calculations of the $|A^\lambda_{tp}|^2$ intensity parameters. It was pointed out in an ab initio study[42] that the neglection of overlap effects could lead to a considerable underestimation of some $|A^\lambda_{tp}|^2$ parameters with $\lambda = 6$, and a overestimation of those with $\lambda = 2$. Accordingly, the calculated vibronic oscillator strengths for the transitions, with large SRMEs of $U^{(6)}$ compared

TABLE 5: Calculated Average Intensity Parameters (in units of 10^{-22} cm^2) for $Cs_2NaNdCl_6$ at 300 K

λ_{tp}	$\langle\lvert A_{tp}^{\lambda}[SC]\rvert^2\rangle$	$\langle\lvert A_{tp}^{\lambda}[DC]\rvert^2\rangle$	$\langle\lvert A_{tp}^{\lambda}\rvert^2\rangle$	λ_{tp}	$\langle\lvert A_{tp}^{\lambda}[SC]\rvert^2\rangle$	$\langle\lvert A_{tp}^{\lambda}[DC]\rvert^2\rangle$	$\langle\lvert A_{tp}^{\lambda}\rvert^2\rangle$
210	207.52	0.00	207.52	455	0.86	13.42	7.71
211	210.87	0.00	210.87	650	15.35	0.00	15.35
230	13.13	83.21	31.22	651	11.57	0.00	11.57
231	8.03	64.12	27.60	652	5.47	0.00	5.47
232	2.28	24.63	11.99	653	8.58	0.00	8.58
233	10.27	73.20	29.61	654	3.57	0.00	3.57
430	72.84	0.00	72.84	655	13.49	0.00	13.49
431	44.55	0.00	44.55	670	0.78	5.97	2.46
432	12.62	0.00	12.62	671	0.56	5.51	2.57
433	56.97	0.00	56.97	672	0.15	1.59	0.78
450	0.98	11.47	6.03	673	0.14	1.10	0.46
451	0.74	13.51	8.07	674	0.10	1.12	0.55
452	0.35	6.70	4.00	675	0.14	1.20	0.54
453	0.55	6.96	3.65	676	0.09	0.98	0.48
454	0.23	4.36	2.61	677	0.62	5.52	2.47

TABLE 6: Vibronic Oscillator Strengths P (10^{-7}) for $Cs_2NaNdCl_6$ at 300 K

group no.	upper levels involved in transition	SC	DC	SC and DC[a]	SC and DC[b]	expt[c]
1	$^4F_{3/2}$	1.39	0.46	1.63	1.62	2.51
2	$^4F_{5/2}$, $^2H_{9/2}$	2.74	1.13	3.15	3.17	7.35
3	$^4F_{7/2}$, $^4S_{3/2}$	1.40	0.53	1.60	1.82	6.02
4	$^4G_{5/2}$, $^2G_{7/2}$	39.14	21.89	45.74	44.61	36.10
5	$^4G_{7/2}$, $^4G_{9/2}$, $^2K_{13/2}$	4.75	2.23	5.54	6.66	10.77
6	$^2G_{9/2}$, $^2D_{3/2}$, $^4G_{11/2}$, $^2K_{15/2}$	0.64	0.23	0.74	0.88	1.92
7	$^2P_{1/2}$	0.48	0.16	0.57	0.57	0.64
8	$^4D_{3/2}$, $^4D_{5/2}$, $^4D_{1/2}$, $^2I_{11/2}$, $^2L_{15/2}$	8.34	2.84	9.73	8.12	7.97

[a] Calculated oscillator strengths without J mixing. [b] Calculated oscillator strengths with J mixing effects included. [c] Reference 15.

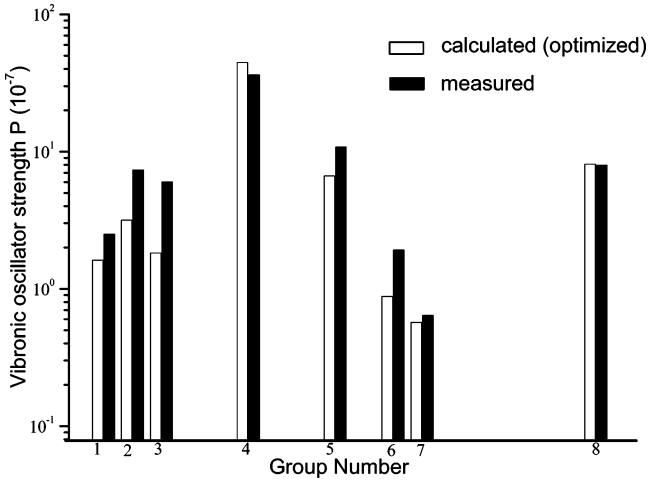

Figure 1. Vibronic oscillator strengths P (10^{-7}) for $Cs_2NaNdCl_6$ at 300 K. For each column, the left bar was calculated using optimized effective charges and the polarizability of the Cl ion, and the other one is measured (ref 15). The group numbers correspond to transition groups shown in Table 6.

to $U^{(2)}$ (see Table 6), are expected to be smaller than the experimental values. This is indeed the case for the second and third groups of transitions in Table 6. The fourth group contains the $^4I_{9/2} \rightarrow {}^4G_{5/2}$ oscillator strength usually referred to as the hypersensitive transition. This transition has a comparatively large SRME value of $U^{(2)}$. The calculated vibronic oscillator strength is, although slightly overestimated, in good agreement with the experimental value. This indicates that the electrostatic model with optimized effective point charges and the isotropic polarizability is appropriate for estimation of the $|A_{tp}^{\lambda}|^2$ ($\lambda = 2$) parameter values. Therefore, a full consideration of the overlap of charge distributions between Nd ions and Cl ions would be needed for further improvement of the theoretical results, in particular for those transitions with comparatively large SRME values of $U^{(6)}$. In addition, it is likely that the inclusion of electron correlation effects could influence the oscillator strengths, especially so for high-energy zero-phonon absorptions.[32] Such correlation effects introduce one- and two-electron effective operators that modify the standard Judd−Ofelt theory, and could thus also alter the calculated vibronic oscillator strengths. Further studies of covalency and correlation effects are in progress.

5. Conclusions

Dynamic intensity model calculations of vibronic oscillator strengths for $Cs_2NaNdCl_6$ have been performed by using MDS. The optimized force parameters used in the MDS reproduce several bulk properties very well. For each MDS-generated environment, both the SC and DC mechanisms were taken into account in the intensity parameter calculations. The self-consistent electrostatic model was applied with optimized point charges and isotropic polarizabilities with respect to experimental energy levels. The calculated vibronic oscillator strengths for the combined SC and DC mechanism agree quite well with the experimental findings. The contributions from the DC mechanism were found to be significant. The J-mixing effect was included which slightly improved the agreement with experiment. Finally, the results have been rationalized by a consideration of the overlap between charge densities of the Nd ion and its neighboring Cl ions. It is our opinion that the dynamic intensity model together with MDS is a very helpful tool in the calculation of vibronic transition intensities. It is simple to apply and avoids derivation of vibrational wave functions or derivatives with respect to normal coordinates. Moreover, it is important to note that the calculation procedure discussed in the present work is general and thus in principle applicable to RE ions in any material, for instance, complex amorphous systems (e.g., glasses).[13]

Acknowledgment. We thank the Swedish Research Council (VR) for supporting this work.

References and Notes

(1) Faulkner, T. R.; Richardson, F. S. *Mol. Phys.* **1978**, *35*, 1141.
(2) Faulkner, T. R.; Richardson, F. S. *Mol. Phys.* **1978**, *36*, 193.
(3) Judd, B.R. *Phys. Scr.* **1980**, *21*, 543.
(4) Stavola, M.; Isganitis, L.; Sceats, N. G. *J. Chem. Phys.* **1981**, *74*, 4228.
(5) Dexpert-Ghys, J.; Auzel, F. *J. Chem. Phys.* **1984**, *80*, 4003.
(6) Wolf, M.; Edvardsson, S.; Zendejas, M. A.; Thomas, J. O. *Phys. Rev. B* **1993**, *48*, 10129.
(7) Edvardsson, S.; Klintenberg, M.; Thomas, J. O. *Phys. Rev. B* **1996**, *54*, 17476.
(8) Brawer, S. A.; Weber, M. J. *J. Chem. Phys.* **1981**, *75*, 3522.
(9) Cormier, G.; Capobianco, J. A.; Morrison, C. A.; Monteil, A. *Phys. Rev. B* **1993**, *48*, 16290.
(10) Monteil, A.; Chaussedent, S.; Capobianco, J. A. *Mol. Sim.* **1997**, *20*, 127.
(11) Klintenberg, M.; Edvardsson, S.; Thomas, J. O. *J. Lumin.* **1997**, *72*, 218.
(12) Edvardsson, S.; Klintenberg, M. *Mater. Sci. Forum* **1999**, *315*, 407.
(13) Edvardsson, S.; Ning, L.; Åberg, D. *J. Phys. B: At. Mol. Opt. Phys.* **2006**, *39*, 2127.
(14) Tofield, B. C.; Weber, H. P. *Phys. Rev. B* **1974**, *10*, 4560.
(15) Strek, W.; Mazurak, Z.; Szafranski, C.; Hanuza, J.; Hermanowicz, K.; Jezowska-Trzebiatowska, B. *Chem. Phys.* **1984**, *84*, 269.
(16) Collombet, A.; Guyot, Y.; Mak, C. S. K.; Tanner, P. A.; Joubert, M. *J. Lumin.* **2001**, *94*/*95*, 39.
(17) Reid, M. F. In *Crystal-field Handbook*; Newman, D. J., Ng, B., Eds.; Cambridge University Press: Cambridge, U.K., 2000; pp 192−224.
(18) Görller-Walrand, C.; Binnemans, K. In *Handbook on the Physics and Chemistry of Rare Earths*; Gschneidner, K. A., Jr., Eyring, L., Eds.; North-Holland: Amsterdam, 1998; Vol. 25, pp 109−164.
(19) Tanner, P. A. *Top. Curr. Chem.* **2004**, *241*, 167.
(20) Meyer, G. *Prog. Solid State Chem.* **1982**, *14*, 141.
(21) Knudsen, G. P. *Solid State Commun.***1984**, *49*, 1045.
(22) Dick, B. J.; Overhauser, A. W. *Phys. Rev.* **1958**, *112*, 90.
(23) Madden, P. A.; Wilson, M. *Chem. Soc. Rev.* **1996**, *25*, 339.
(24) Gale, J. D.; Rohl, A. L. *Mol. Simul.* **2003**, *28*, 385.
(25) Sangster, M. J. L.; Atwood, R. M. *J. Phys. C: Solid State Phys.* **1978**, *11*, 1541.
(26) Ning, L.; Tanner, P. A.; Xia, S. *Vibr. Spectrosc.* **2003**, *31*, 51.
(27) Gale, J. D. *Philos. Mag. B* **1996**, *73*, 3.
(28) Reid, M. F.; Richardson, F. S. *J. Chem. Phys.* **1983**, *79*, 5735.
(29) Judd, B. R. *Phys. Rev.* **1962**, *127*, 750.
(30) Åberg, D.; Edvardsson, S. *Phys. Rev. B* **2002**, *65*, 045111.
(31) Faucher, M.; Garcia, D. *Phys. Rev. B* **1982**, *26*, 5451.
(32) Åberg, D.; Edvardsson, S.; Engholm, M. *Phys. Rev. B* **2003**, *68*, 195105.
(33) Richardson, F. S.; Reid, M. F.; Dallara, J. J.; Smith, R. D. *J. Chem. Phys.* **1985**, *83*, 3813.
(34) Edvardsson, S.; Åberg, D. *Comput. Phys. Commun.* **2001**, *133*, 396.
(35) Schmidt, P. C.; Weiss, A.; Das, T. P. *Phys. Rev. B* **1979**, *19*, 5525.
(36) Peacock, R. D. *Struct. Bonding (Berlin)* **1975**, *22*, 83.
(37) Xia, S.; Reid, M. F. *J. Phys. Chem. Solids* **1993**, *54*, 777.
(38) Malta, O. L.; Couto dos Santos, M. A.; Thompson, L. C.; Ito, N. K. *J. Lumin.* **1996**, *60*, 77.
(39) Malta, O. L.; Carlos, L. D. *Quim. Nova.* **2003**, *26*, 889.
(40) Tanner, P. A. Private communication, 2005.
(41) Xia, S.; Chen, Y. *J. Lumin.* **1985**, *33*, 228.
(42) Reid, M. F. In *Spectroscopic Properties of Rare Earths in Optical Materials*; Liu, G., Jacquier, B., Eds.; Tsinghua University Press: Tsinghua, China, 2005; pp 117−121.